CONEM 2016 CONGRESSO NACIONAL DE ENGENHARIA MECÂNICA
21 - 25 AGOSTO DE 2016 FORTALEZA - CEARÁ

BEHAVIOR OF TEMPERATURE GRADIENTS IN FUEL OIL EXPORTATION THROUGH A 12 INCHES PIPE UNDER INVISCID AND VISCOUS CONDITIONS

Flavio Peres Amado, flavioam@petrobras.com.br, fpamado@live.estacio.br
Ediomedson Sales de Lucena, sales@dhn.mar.mil.br, ediomedson@hotmail.com
Mila R. Avelino, mila.avelino@pq.cnpq.br, mila.avelino@gmail.com
Universidade Estácio de Sá, Eng. Mecânica, R. Eduardo Luiz Gomes 134, Niterói, Postal code 24020-340, RJ, Brazil
Universidade Estácio de Sá, Eng. Mecânica, R. Eduardo Luiz Gomes 134, Niterói, Postal code 24020-340, RJ, Brazil
Universidade Estácio de Sá, Eng. Mecânica, R. Eduardo Luiz Gomes 134, Niterói, Postal code 24020-340, RJ, Brazil

CON-2016-0026

***Abstract**: Inviscid flows have been reference for viscous flow. In this work a comparison of results from a flow between a refinery and a distribution terminal in Brazilian Northeastern region is performed. Results for viscous and inviscid conditions, in laminar regime are likened. Simulations were implemented using the finite difference method. A commercial code that works with finite element method was performed as additional comparison source. Results show that viscosity behaved as a factor of heat keeping and made the fluid's temperature less sensible to the lack of piping insulation. Some thermal instability is noted for the inviscid conditions at the inner wall of the insulated piping and it is concluded that it might have been caused by the lack of insulation and thickness reduction of a posterior stretch.*

***Keywords:** Temperature Gradients, Viscosity*

1. INTRODUCTION

Inviscid flow with consequent constant velocity are useful because constitute ideal conditions that serve as reference for calculus in real behavior for the various flowing phenomena, such as those inside a piping, heating/cooling process, aeronautics, acoustics, and so on.

As instances, Ozaki et al (1978) researched a flow of a gas motion in a rotating cylinder induced by a forced source-sink. Flow was measured using a laser Doppler anemometer in connection with the development of a gas centrifuge for 235U enrichment. In a time when there was not a computational resource to treat Navier-Stokes equations as of today, it was shown that the viscosity was important only within the thin boundary layers: the Ekman layers on the upper and lower end plates and the Stewartson layers on the side wall and in the cylinder, if there was a forced source sink flow.

In terms of dynamic instability, Bogdevičius (2003) has modeled a rotating pipe conveying fluid. The non-linear equation of the pipe's motion was derived using the finite element method. In his study, he considered the fluid as incompressible and inviscid one. He obtained the one-third sub-harmonic amplitudes of the rotating cantilevered pipe conveying fluid and concluded that those amplitudes depend on fluid pressure, flow velocity and angular velocity in inviscid conditions.

Williams (2007) presented a surface adaptive curvilinear finite volume method for solving free-surface flows. Code verification was carried out on a number of inviscid, laminar and turbulent flow cases and the results showed good agreement with experimental data and theoretical solutions.

Madadi et al (2015) developed a work about boundary conditions in equations governing inviscid fluid flow. In that article, four different methods for calculation of the wall velocity magnitude were introduced, tested and compared against several test cases of subsonic and supersonic flows. Since there are many problems where both subsonic and supersonic flows coexist, a mixed boundary condition taking into account the flow Mach number was proposed. For subsonic and transonic flow the third type (density x velocity magnitude = cte) has better accuracy than the others. For supersonic flows, the second type (velocity magnitude = cte) showed better accuracy. A combination of the second and third type of flow regimes called "the mixed boundary condition" was tested in two test cases of both subsonic and supersonic flow regimes. The results showed that this condition was applicable with good agreement.

In aeronautics, Maciel (2007) has tested the Euler and Navier-Stokes equation in three dimensions through Jameson and Mavriplis and the Liou and Steffen unstructured algorithms for wind tunnel testing simulation. The results demonstrated that both schemes predicted appropriately the shock angles at the ramp and at the lower and upper wallsof of the diffuser, in the inviscid case. In the viscous study, only the Liou and Steffen scheme yielded converged results, obtaining good ramp shock angles.

Lasauskas and Naujokaitis (2009) analyzed three wing sections in lift condition in three different research centers. They perform codes as Eppler, XFOIL and RFOIL. Eppler's code uses non-interacted inviscid plus boundary layer method. Influence of separation is estimated using empirical correction in this method. XFOIL code uses interacted zonal viscous/inviscid method. RFOIL is a modification of XFOIL code for application in wind turbines. Their conclusions were that calculation predicted well the range of lift coefficient for low drag. In the low drag range the predicted drag was about from 10 % to 20 % lower than measured drag. Eppler's code predicted drag in low drag region better than XFOIL and RFOIL. Eppler's code overpredicted momentum coefficient and couldn't predict maximum lift and lift curve in post stall region. At low Reynolds numbers the experimental lift curve was about in the middle between XFOIL prediction and RFOIL prediction in the post stall region. At high Reynolds number XFOIL code overpredicted maximum lift and the lift in post stall region. RFOIL code predicted lift curve very well even in post stall region. Both XFOIL and RFOIL codes predicted the pitching moment curve including post stall regime.

In astrophysical fluid dynamics, Zhen et al (2014) treated to solve an important unanswered mathematical question in the theory of rotating fluids that has been the completeness of the inviscid eigenfunctions which are usually referred to as inertial waves or inertial modes. They provided for the first time a mathematical proof for the completeness of the inertial modes in a rotating annular channel by establishing the completeness relation, or Parseval's equality, for any piecewise continuous, differentiable velocity of an incompressible fluid.

Acoustics have been also studied in inviscid conditions. In fact, the viscosity of the medium together with its thermal conductivity are partially responsible for the natural attenuation of sound waves. Abd-El-Malek and Hanna (1997) developed a mathematical model to describe the physical effect of viscosity of a medium and the wave number on sound propagation and sound attenuation numbers, in circular ducts. They concluded that the propagation number is a weak function of Reynolds Number *(Re)* and that as *Re* increases, the propagation number tend to the value in inviscid condition. For all practical purposes, the effect of viscosity can be neglected on the wave propagation. They also concluded that the medium viscosity has a noticeable effect on the attenuation numbers and low Reynolds numbers.

Viscosity is a main input for flow hydraulic models due to the fact that the choice of the flow regime equations (laminar, transition or turbulent) relies on it. Besides that, from the hydraulic point of view, the absolute and kinematic viscosities of generic liquids can be modeled using two or three parameters and the liquid's temperature. Santana et al (2005) addressed this issue by adjusting equations using a non-linear regression and suggested expressions that best fit the data were used, which were obtained to represent the entire range of variation of the viscosity for petroleum products. They observed that three parameters equations are best suited for the curves and therefore are more appropriated for hydraulic models. Classically, it is known that viscosity decreases as temperature increases, but keep fluids warmer and it was confirmed by their work.

Following this path of comparison between viscous and inviscid condition of flow, a research of the behavior of temperature gradients, relative to a fuel oil transported from a refinery toward a distribution terminal, in Brazilian Northeastern Region, with some particular characteristics, is performed. The piping presents the inner wall's design temperature of 353 K and has a loss of thermal energy in a stretch of 30 meters where there is a reduction of ½ inch in thickness and no thermal insulation.

As starting point, it was carried out a study by Ciambeli and Fonseca (2014) to figure out radial temperature gradients that considered ideal condition of viscosity and flow's velocity. That work was made by the aid of a commercial code, not an independent mathematical modeling.

Herein it is proposed a more accurate gradient calculation by inserting the thermal-dependent viscosity and a more realistic profile of the flow's velocity as important parcels of the energy equation. Additionally, it was modeled an inviscid flow with a consequent constant velocity profile to compare to that approach. Mathematical models were implemented in finite difference method and are pretty similar

2. BIBLIOGRAPHIC BASIS FOR THIS WORK

Equations governing phenomena are inside the well-known Eq. (1), that might be taken from the vast specialized literature (Chapman 1984; Bejan 1993; Holman 1999; Çengel and Cimbala 2015), and that can be found below in cylindrical coordinate:

$$\frac{1}{r}\frac{(\partial kr\left(\frac{\partial T}{\partial r}\right))}{\partial r}+\frac{1}{r^2}\frac{(\partial k\left(\frac{\partial T}{\partial \theta}\right))}{\partial \theta}+\frac{(\partial k\left(\frac{\partial T}{\partial z}\right))}{\partial z}+\mu'''=\rho c\left(\frac{DT}{Dt}\right)+\mu\Phi \tag{1}$$

where μ is the dynamical viscosity and Φ is an expression of partial derivatives that takes in account velocities according the following way:

$$\Phi = 2\left[\left(\frac{\partial v_r}{\partial r}\right)^2 + \left(\frac{1}{r}\frac{\partial v_\theta}{\partial \theta} + \frac{v_r}{r}\right)^2 + \left(\frac{\partial v_z}{\partial z}\right)^2\right] + \left(\frac{\partial v_\theta}{\partial r} - \frac{v_\theta}{r} + \frac{1}{r}\frac{\partial v_r}{\theta}\right) + \left(\frac{1}{r}\frac{\partial v_z}{\partial \theta} + \frac{\partial v_\theta}{\partial z}\right)^2 + \left(\frac{\partial v_r}{\partial z} + \frac{\partial v_z}{\partial r}\right)^2 \tag{2}$$

Obviously that, for an inviscid flow, Eq. (2) will be discarded as well as some parts of Eq. (1). Additionally, if it is approaching a laminar regime in a straight pipe with constant physical properties, Navier-Stokes equation can be reduced and expressed in cylindrical coordinates according the Eq. (3).

$$0 = -\frac{\partial P}{\partial z} + \mu\frac{1}{r}\frac{\partial}{\partial r}\left(r\frac{\partial v_z}{\partial r}\right) \tag{3}$$

For a viscous flow, the solution for v_z will be:

$$v_z = \frac{2Q}{\pi r_i^4}\left(r_i^2 - r^2\right) \tag{4}$$

Where Q is the flow rate and r_i is the inner radius of the pipe.

Nevertheless, for a condition that discards the variation of the velocity profile in a laminar flow, this variable can be calculated solely through Eq. (5):

$$v_z = \frac{Q}{A} \tag{5}$$

Where A is the inner area of the pipe's transversal section.

3. MATERIALS AND METHODS

Infrastructure serving as a basis for this study is a pipe line that links a refinery to the distribution terminal that was built in 1977. It has nominal diameter, D_i, 0.3048 m (12 inches), thickness 0.0127 m (½ inch) and 35100 m (35.1 km) of extension, L. There is a stretch of interest of 1080 meters. This length contemplates 1020 meters of insulated pipe, plus 30 meters non-insulated, between two points, 1 and 2 according Fig. 1, and a final insulated stretch of 30 meters, from which the pipe buries into the ground. A problem of thermal energy loosing occurs internally, between points 1 and 2, where there is a reduction of thickness to 6,4 mm and two in-situ measurements were carried out.

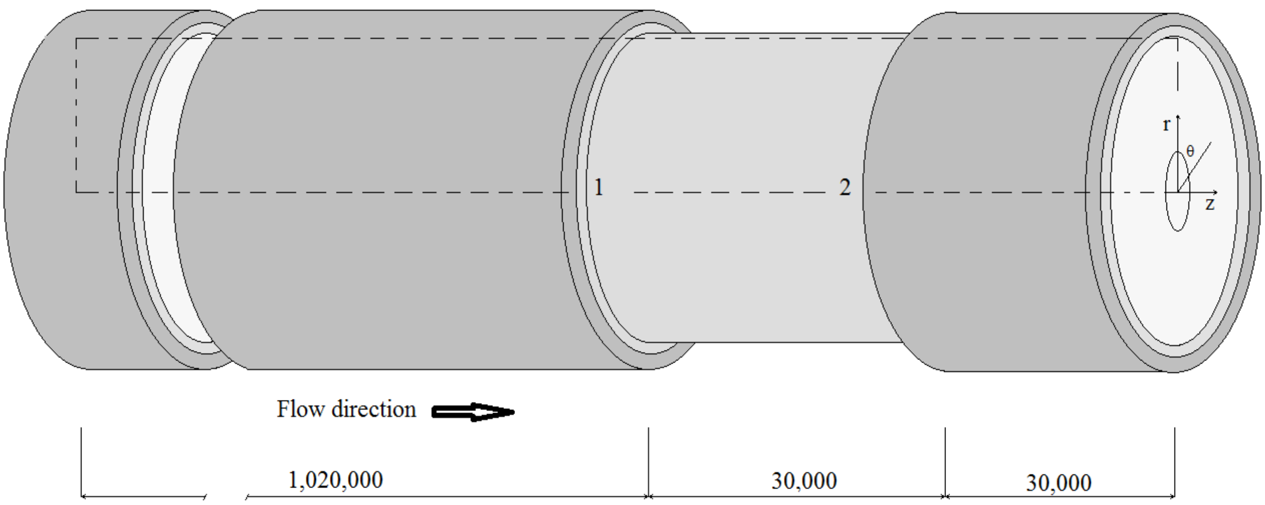

Figure 1 – Sketch of part of the pipeline that links the refinery and the distribution terminal. The simulated area is a 2D plan at the superior half of the inner region.

3.1. Properties and general data of the fluid

Ciambeli and Fonseca (2014), informed all physical properties of fuel oil and the infrastructure of transportation that this work demands to perform the simulation. Properties of the pipe and insulation materials can be found in Tab. 1.

Table 1 – Properties of pipe and insulation materials

Lenght (m)	Tickness (mm)	kpipe (W/mK)	Insul. Tick. (mm)	kinsul (W/mK)
1,020	12.7	46	50.8	0.03
30	6.4	46	-	-

In terms of flow rates, this work simulated 0.04 m^3/s (150 m^3/h) and 0.07 m^3/s (250 m3/h).

Other relevant properties to the formation of radial gradient and to compute the drop of the temperature along the flowing process are fuel oil's thermal conductivity k_{fluid} and the specific heat c_p. Ciambeli and Fonseca (2014) utilized results from the study made by Czubinski et al (2013) where they have measured these properties in five different types of oil. They verified that such properties are similar for different cases. Thus, chosen values were k_{fluid} = 0.137 W/mK and c_p = 1970 J/kgK.

Relatively to the density ρ and viscosity μ, Ciambeli and Fonseca (2014) recommend 937.4 kg/m3 and 506 kg/ms, respectively.

At last, the outer film coefficient h existing between the pipe's hull and the exterior environment was informed as being 1.3 W/m2K and the inner film coefficient was calculated according Eq (6).

$$h = \frac{k_{fluid}}{D_i}\left\{\frac{3.66+0.0668R_e\left(\frac{c_p\mu}{k_{fluid}}\right)\frac{D_i}{L}}{1+0.04\left[R_e\left(\frac{c_p\mu}{k_{fluid}}\right)\frac{D_i}{L}\right]^{2/3}}\right\} \tag{6}$$

3.2. Dimensionless Values

Taking in account all physical properties and geometric characteristics, Reynold number resulted around 0,5 and Nusselt number was not higher than 5. Because of the high values of c_p and μ and low k_{fluid} value, Prandtl number resulted to be very high.

3.3. Mathematical Modeling and Assumptions

Assumptions to Eq. (1) and Eq. (2) for inviscid flow were imposed according following items: There is no energy generation, there are no tangential gradients, fluid's thermal conductivity, density, specific heat and velocity profile are constants. These restrictions resulted in Eq. (7):

$$\frac{1}{r}\frac{\left(\partial kr\left(\frac{\partial T}{\partial r}\right)\right)}{\partial r} + \frac{\left(\partial k\left(\frac{\partial T}{\partial z}\right)\right)}{\partial z} = \rho c\left(\frac{\partial T}{\partial t} + v_z\frac{\partial T}{\partial z}\right) \tag{7}$$

By the association of Eq. (5) and Eq. (7), it will be achieved the Eq. (8) that describes the complete mathematical model of the fuel oil's thermal behavior in terms of inviscid conditions:

$$\frac{1}{r}\frac{\partial T}{\partial r} + \frac{\partial^2 T}{\partial r^2} + \frac{\partial^2 T}{\partial z^2} - \frac{Q}{kA}\frac{\partial T}{\partial z} = \frac{\rho c}{k}\frac{\partial T}{\partial t} \tag{8}$$

The model that describes the viscous flow under the same assumption is quite a bit more complicated. It is necessary to associate Eq. (1), Eq. (2) and Eq. (4). This "blend" can be found as Eq. (9):

$$\frac{1}{r}\frac{\partial T}{\partial r} + \frac{\partial^2 T}{\partial r^2} + \frac{\partial^2 T}{\partial z^2} - \frac{2\rho c Q(r_i^2 - r^2)}{k\pi r_i^4}\frac{\partial T}{\partial z} - \mu\left(\frac{4Qr}{\pi r_i^2}\right)^2 = \frac{\rho c}{k}\frac{\partial T}{\partial t} \tag{9}$$

That said, Eq. (8) and Eq. (9) were discretized in finite difference method and implemented in computational language to simulate the thermic flow in order to figure out the gradients in z and r, inside the region of interest. Simulation scheme can be found in Tab. 2.

Table 2 – Simulation scheme

Parameter	radius	Insulated stretch	Non-insulated stretch	Appendix	Steps of time
intervals	25	102	30	5	10^{-5}
Total of nodes	3425				

It was chosen a flowing of 350 seconds long, which represents the interval of time that the central line of fuel oil takes to achieve the region without insulation.

The convergence criterion was 10^{-8} compared to the relative error and only one simulation with step of 10^{-6} seconds was carried out. Considering that results were similar from those obtained with steps of 10^{-5} seconds and that this simulation required considerable computational effort, it was discarded.

3.4. Initial and boundary conditions

Initial conditions of temperature, flow rates and mathematical assumptions for boundary conditions, in order to solve Eq. (8) and Eq. (9), can be found in Tab. 3. As equations result in symmetry of flowing conditions, the half of any longitudinal section is representative of the whole inner tube.

Table 3 – Boundary conditions and flow rates for Eq. (8) and Eq. (9)

Parameter	Simulation 1	Simulation 2	Simulation 3
Initial temperature Ti	348 K	353 K	353 K
Environ. temperature	308 K	308 K	308 K
Flow rate	150 m3/h	150 m3/h	250 m3/h
For r = inner and outer radius	hΔT=-k(dT/dr)	hΔT=-k(dT/dr)	hΔT=-k(dT/dr)

4. RESULTS AND DISCUSSION

Simulations in finite difference method and through the commercial code were made for the setting up of all gradients along the inner wall of the pipe, as well as along the radius, for viscous and inviscid flow. Fig. 2a, b and c and Fig. 3a, b and c show 2D thermal profiles. Fig. 2a, b and c present results of temperature distribution built by the commercial code in inviscid case. Fig. 3a, b and c present the temperature distribution obtained according the herein proposed model, both for inviscid and viscous conditions. In these situations, temperatures profile distribution is confined at the r x z plane.

Figures 4a, b and c show analogous 3D thermal surfaces developed with the herein proposed mathematical models. All results worked respectively in conditions of T_i = 353 K and flow rate = 0.04 m^3/s, T_i = 353 K and flow rate = 0.04 m^3/s and T_i = 353 K and flow rate = 0.07 m^3/s.

Figure 5a, b and c shows a comparison between the various longitudinal gradients for the same conditions above, both for inner wall as for the adjacent layer of fuel oil, nearby the wall. Two in-situ measurements at the wall provided by refinery's personnel can be seen only on the first condition of simulation.

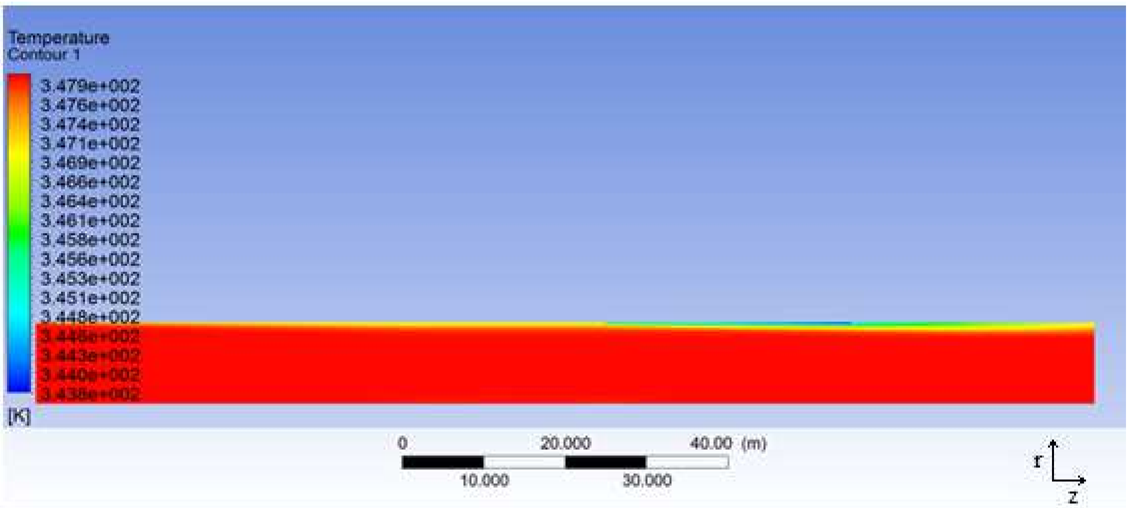

Figure 2a – Temperature distribution in plane r x z, according the commercial code for a length of 130 meters, showing the coldest region in blue, in the nearest portion around the wall of the non-insulated stretch for T_i = 348 K and flow rate = 0.04 m^3/s.

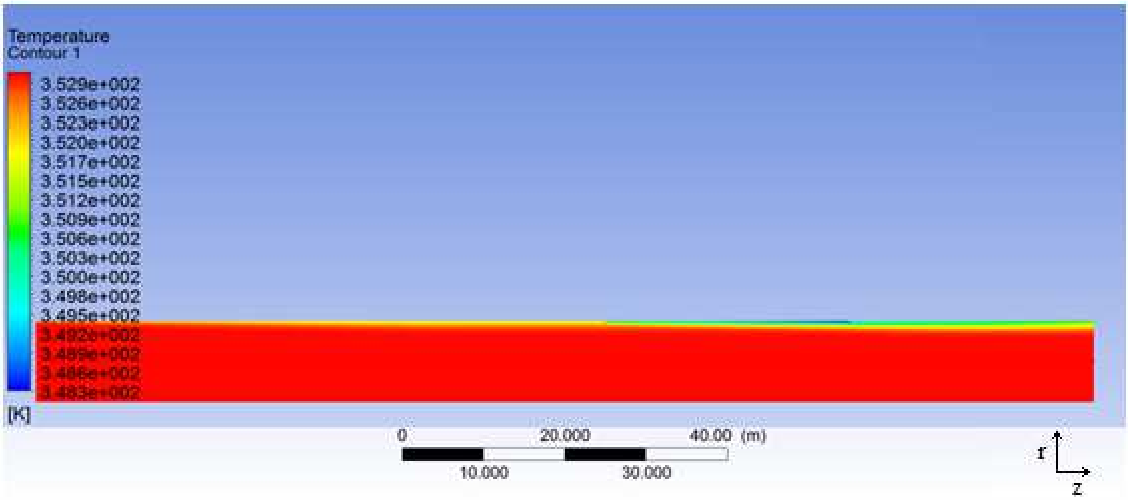

Figure 2b – Temperature distribution in plane r x z, according the commercial code for a length of 130 meters, showing the coldest region in blue, in the nearest portion around the wall of the non-insulated stretch for T_i = 353 K and flow rate = 0.04 m^3/s

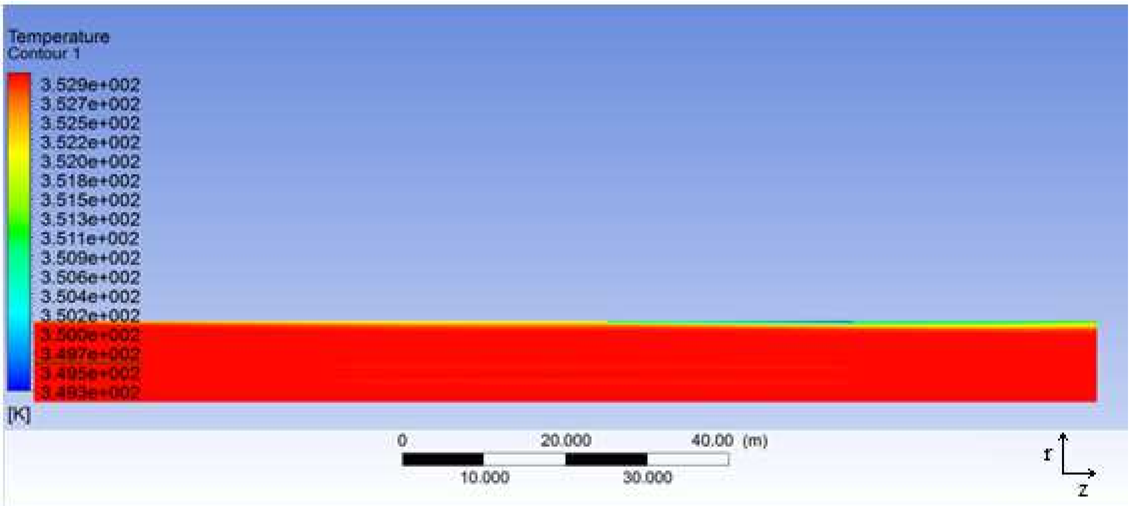

Figure 2c – Temperature distribution in plane r x z, according the commercial code for a length of 130 meters, showing the coldest region in blue, in the nearest portion around the wall of the non-insulated stretch for T_i = 353 K and flow rate = 0.07 m^3/s.

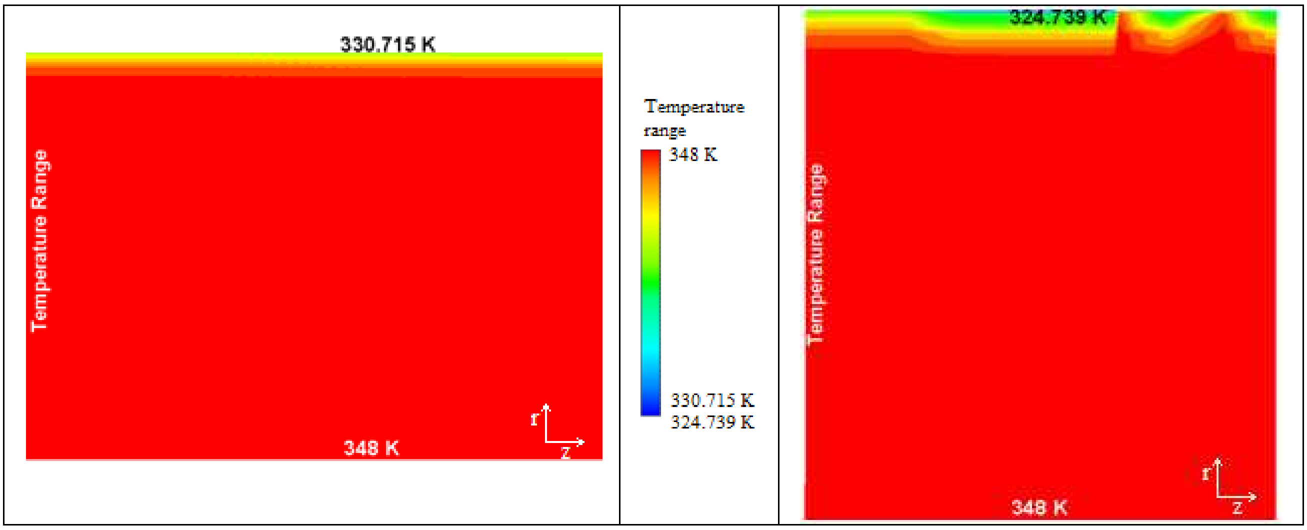

Figure 3a – Temperature distribution in plane r x z, according the herein proposed model, showing the coldest region in blue, in the inner wall of the non-insulated stretch. At left, in viscous conditions and at right, in inviscid conditions for T_i = 348 K and flow rate = 0.04 m^3/s.

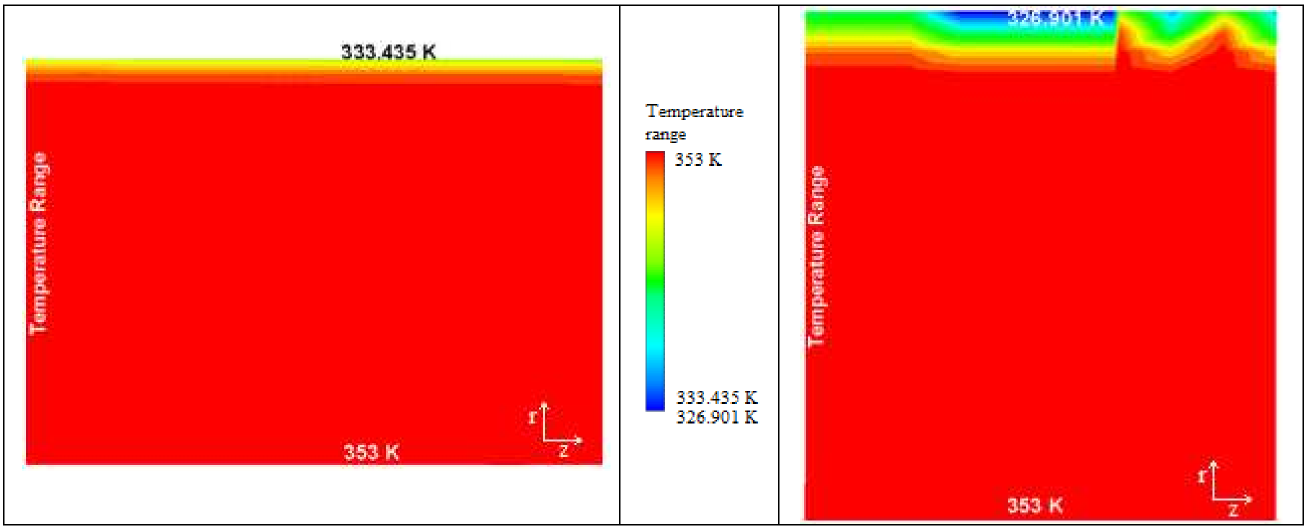

Figure 3b – Temperature distribution in plane r x z, according the herein proposed model, showing the coldest region in blue, in the inner wall of the non-insulated stretch. At left, in viscous conditions and at right, in inviscid conditions for T_i = 353 K and flow rate = 0.04 m^3/s

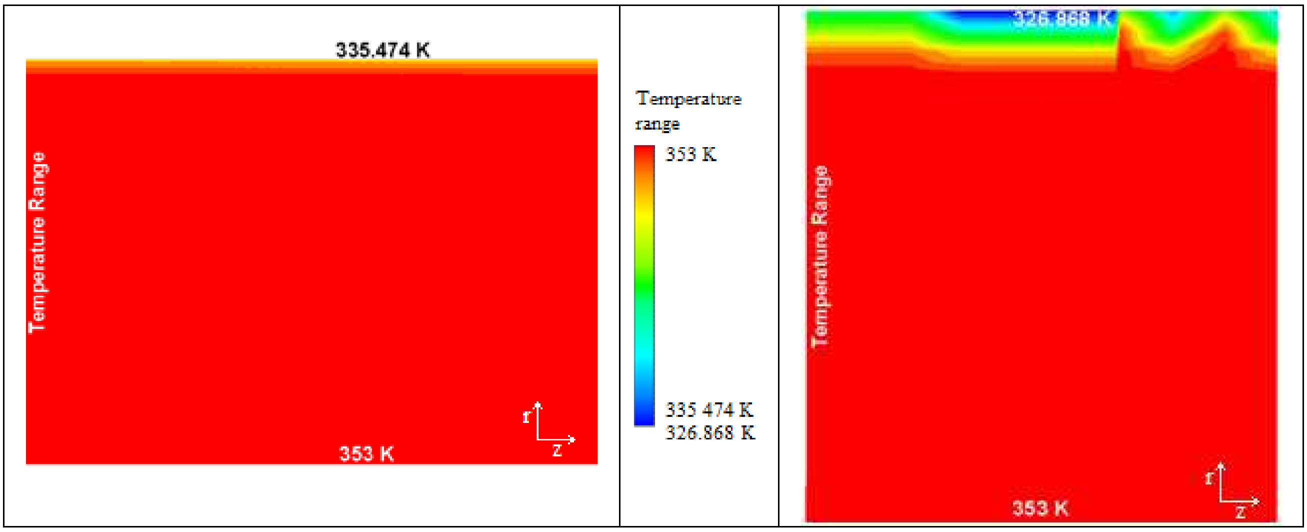

Figure 3c – Temperature distribution in plane r x z, according the herein proposed model, showing the coldest region in blue, in the inner wall of the non-insulated stretch. At left, in viscous conditions and at right, in inviscid conditions for T_i = 353 K and flow rate = 0.07 m^3/s.

2D Surfaces that can be seen in Fig. 2a, b and c and Fig. 3a, b and c are not so enlightening as those in Fig. 4a, b and c. The commercial code shows a drop of temperature that varies between 3.6 and 4,1 degrees centigrade according each specific condition of flowing. 2D surfaces from the herein proposed model for inviscid condition shows a higher drop in the region without insulation, that increases as initial temperature and flow rate increase. There is an apparent anomalous range of temperature between center fillet and the wall temperatures.

On the other hand, a comparison between 3D surfaces in Fig. 4a, b and c shows important differences between thermal behavior of inviscid and viscous flows for the studied cases. First of all, surfaces at right (inviscid ones) show a region of thermal instability before the non-insulated region, that one cannot know if it is caused by some numerical instability of the simulation method or by some physical phenomenon associated, belonging to the flowing. Dravid et al (1971) as well as Akiyama and Cheng (1974) were the first to report such a phenomenon, although in toroidal tubes entrances.

The first work considered a physical behavior of the flow and Akiyama and Cheng (1974) considered that those oscillations are results of numerical instability. Actually, it has to be observed that in the absence of viscous forces that could press a layer of fluid together the inner wall of the pipe, or that could proportionate a back flow phenomenon, the fluid theoretically flows free and might suffer some type of irregular cooling. In respect to this instability, Santana (1997) addressed the issue relatively to the Nusselt Number in curved tubes entrances, in the region of not fully developed flow. In his thesis, he attributed these thermal instabilities to the centrifugation and to vortexes of velocity arising from characteristics of the boundary layer. At a first approach, the phenomenon cannot be associated with that seen herein, because the flow is considered to be fully developed, the stretch is not curved, and more important: there are no effects of boundary layers since the flow is considered inviscid and the velocity is constant. However, this is a process with high Prandtl number as those described above. Moreover, the reduction of thickness of the non-insulated stretch, as well as the lack of insulation itself might be influencing the previous thermal behavior, doing it similar to that described by references above. After the non-insulated stretch, the phenomenon is not observed anymore, as can be observed in figure 4a, b, and c, at right column.

Another important remark is that about the plateau (horizontal region in red) before the drop of temperatures in the vertical region (red to blue region), nearby the inner wall of the tube. In viscous flow, this plateau was larger than that in inviscid flow. Beyond that, when the flow rate increased, this plateau increased as well, ie., radial gradients in viscous flow showed that a larger internal region kept itself warmer for a longer period of time. Oppositely, in inviscid flow, the horizontal plateau's size increased with the initial temperature's augmentation, but not with the flow rate's increase. The vertical region was higher in all presented cases. Viscosity is thus concluded to have behaved as a factor of heat keeping for this fuel oil. Although, there is an inverse mathematical proportion between viscosity and temperature, the more viscosity increases, the more conductivity decreases and this seems to have been the case, as stated in Santana elt al (2005).

Appraising Fig. 5a, it can be seen that results of best coincidence with in-situ measurements were those from inviscid flow for the layer of oil nearby the wall, through the simulation herein proposed. For wall temperature, the best agreement was that for viscous flow, again obtained through the herein proposed model. This fact shows that for these characteristics of flowing, viscosity was no pretty influential on the mathematical modeling.

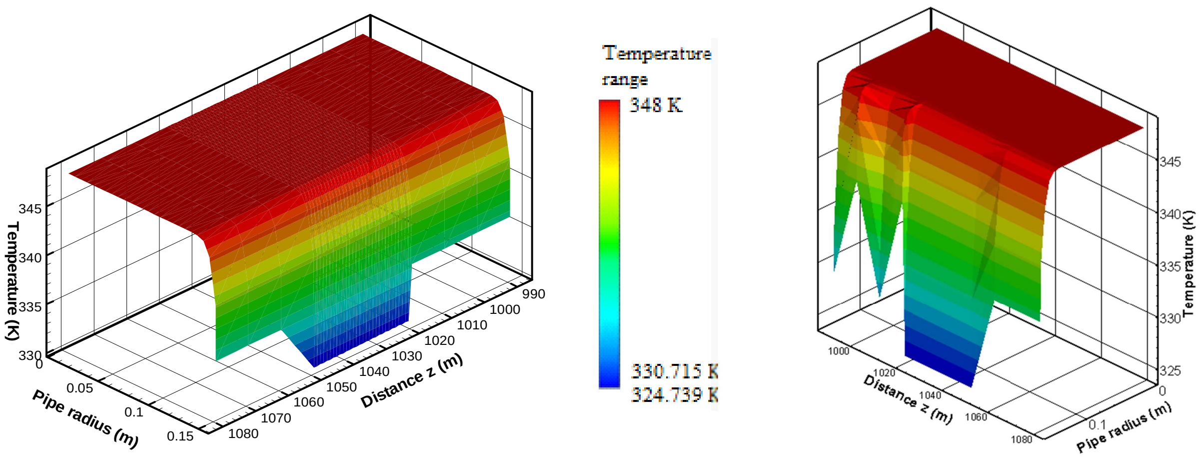

Figure 4a – 3D thermal surfaces, showing temperature gradients in planes r x T and z x T, predicted by finite difference method. At left, in viscous conditions and at right, in inviscid conditions, for Ti = 348 K and flow rate = 0.04 m3/s.

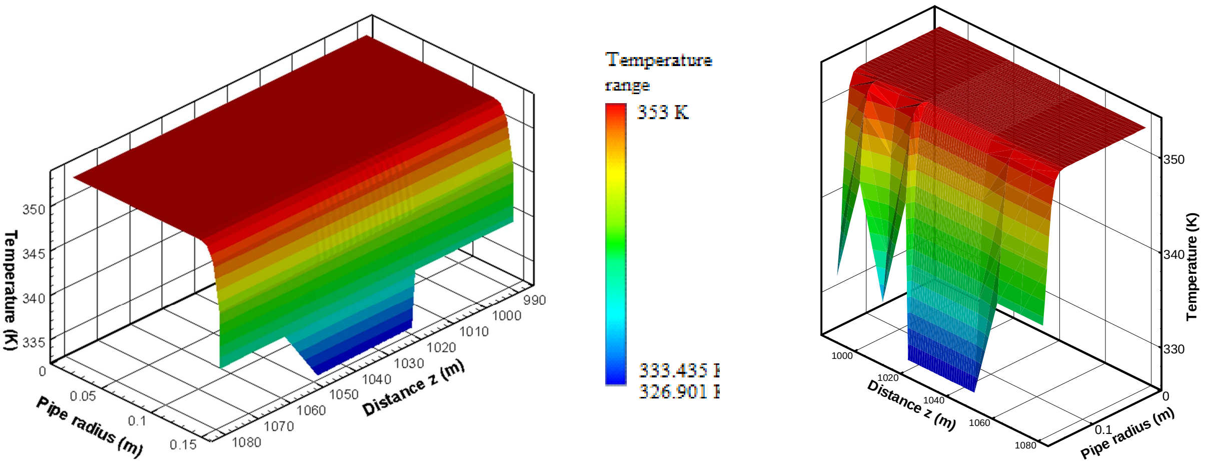

Figure 4b – 3D thermal surfaces, showing temperature gradients in planes r x T and z x T, predicted by finite difference method. At left, in viscous conditions and at right, in inviscid conditions, for Ti = 353 K and flow rate = 0.04 m3/s.

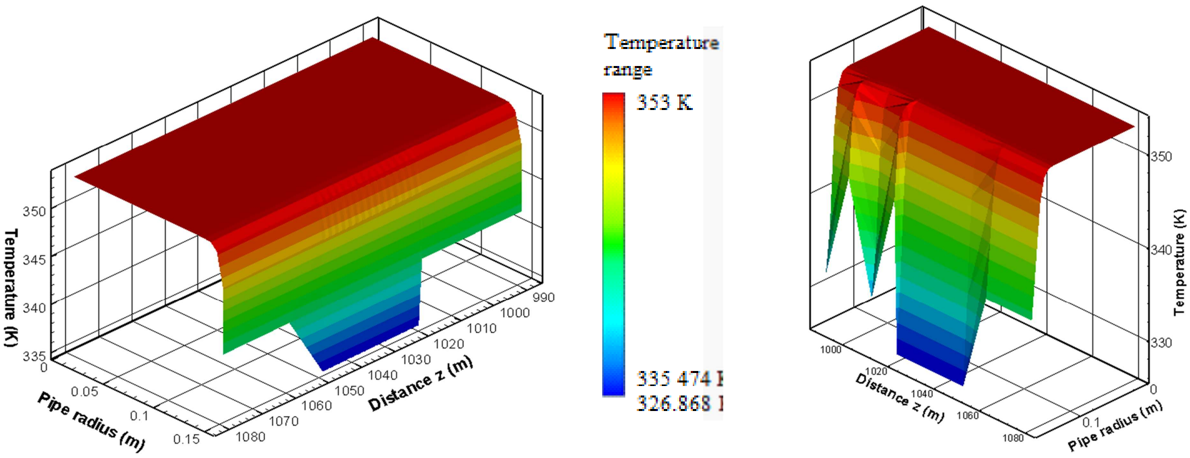

Figure 4c – 3D thermal surfaces, showing temperature gradients in planes r x T and z x T, predicted by finite difference method. At left, in viscous conditions and at right, in inviscid conditions, for T_i = 353 K and flow rate = 0.07 m^3/s.

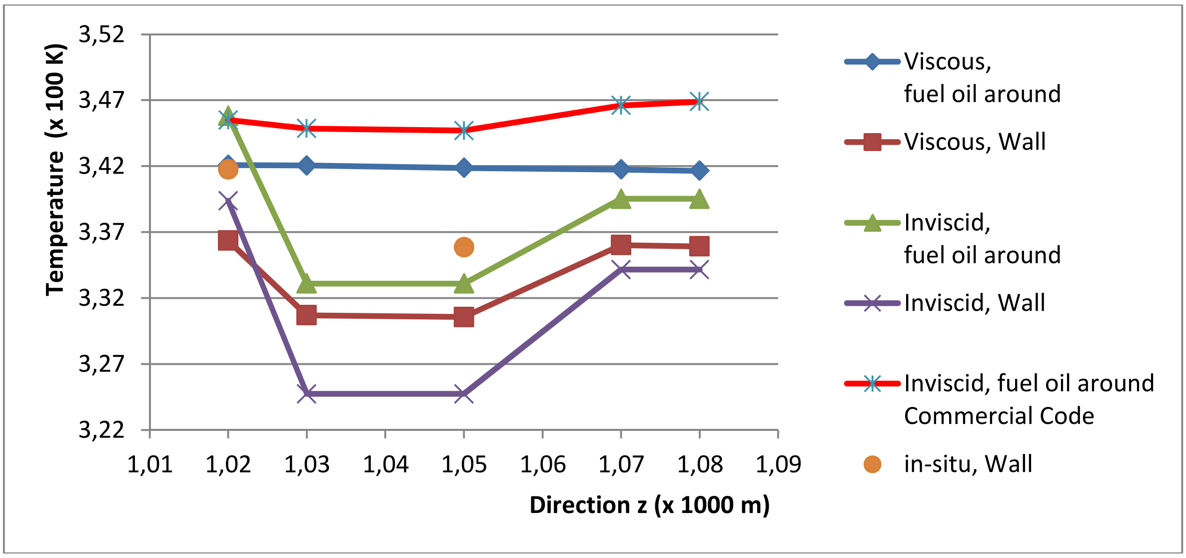

Figure 5a – Comparison between longitudinal gradients for viscous and inviscid conditions on the wall and in layers of fuel oil nearby the wall, according the various sources, for for T_i = 348 K and flow rate = 0.04 m^3/s.

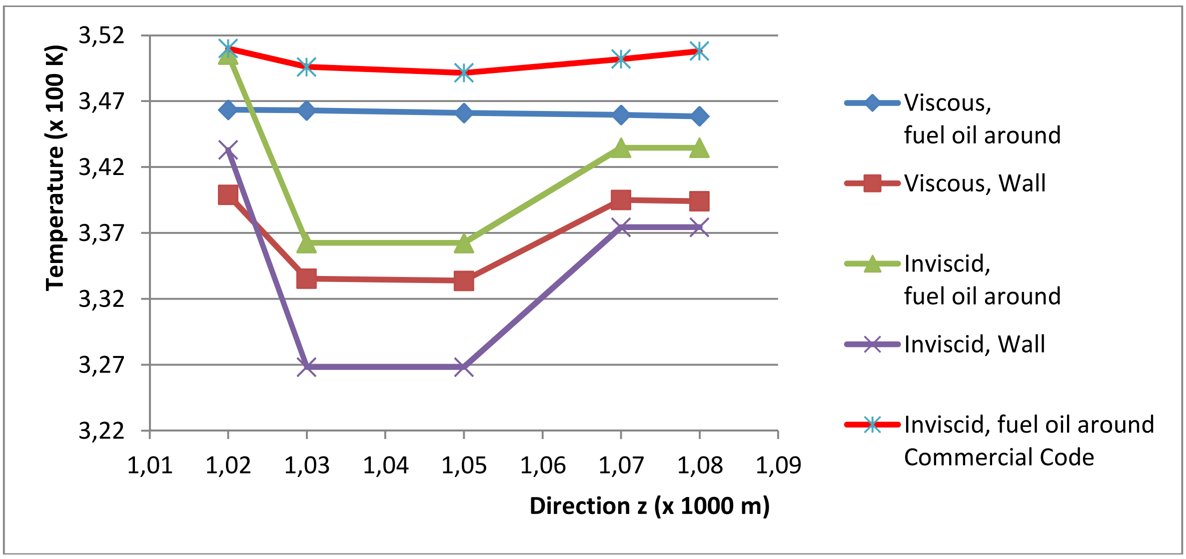

Figure 5b – Comparison between longitudinal gradients for viscous and inviscid conditions on the wall and in layers of fuel oil nearby the wall, according the various sources, for T_i = 353 K and flow rate = 0.04 m^3/s.

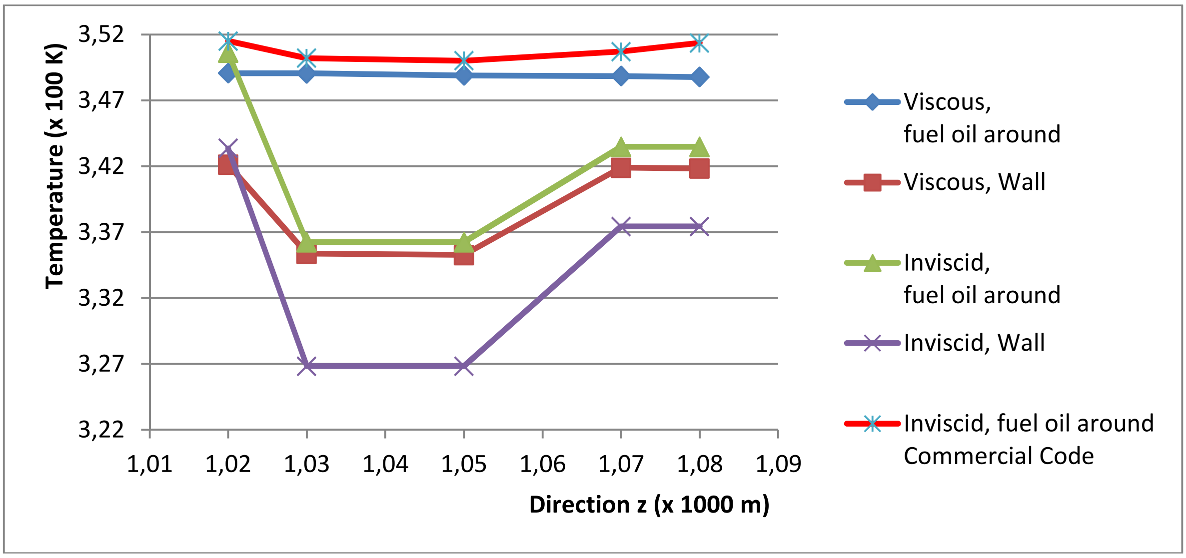

Figure 5c – Comparison between longitudinal gradients for viscous and inviscid conditions on the wall and in layers of fuel oil nearby the wall, according the various sources, for T_i = 353 K and flow rate = 0.07 m^3/s.

Comparison between those three graphics from Fig. 5a, b and c, evincing longitudinal gradients localized inside the non-insulated stretch and nearby the inner wall, indicates that once more the inviscid flow was sensible to the initial temperature's increase, but not to the variation of the flow rate. Temperature values between flow rates of 0.04 m^3/s and 0.07 m^3/s were very similar. The variation was not considerable on the region before the non-insulated stretch. In fact, for inviscid flow the gradient sensibility to the flow rate's increase is not so evident. It can be seen from Eq. (9) that the flow rate Q is multiplied by a parcel of variation of temperature as a function of z. This parcel has a negative value and performs a reduction on the final value of the temperature. Nonetheless, this reduction is significantly small and such a fact resulted in similar thermal surfaces for the two studied flow rate conditions.

Inviscid flow simulation predicted a drop of temperature higher than that for viscous flow along the axial direction. Through the longitudinal gradient's analysis, as well as that observed in radial gradients, viscosity seemed promoting a type of greenhouse effect inside the piping. The middle of the viscous flow kept itself warmer than the periphery, which tended to cool less than in inviscid condition, both in insulated and non-insulated stretches. In Fig. 5a, b and c, gradients shown in blue evinces the phenomenon, ie due to viscosity, the temperature of this fuel oil, a little bit far from the wall, is higher than the equivalent one in inviscid condition. It can be explained in part because the viscous forces link a first layer of fuel oil on the inner wall and give a parabolic profile to the velocity. This adhered layer of oil to the inner wall serves as insulation for inner layers, making them warmer for a longer period of time and in a larger volume. A comparison of these results with that obtained by Abd-El-Malek and Hanna (1997) shows that viscosity of the medium together with its thermal conductivity are partially responsible both for the natural attenuation of sound waves as for the decrease in heat losses.

5. CONCLUSIONS

Inviscid and viscous flow simulations were presented as representatives of the transportation of a fuel oil between a refinery and a distribution terminal in Brazilian Northeastern. Mathematical models were implemented in finite difference method and covered three combinations of conditions of flow rate and initial temperature. A simulation in a commercial code was performed as well, in order to compound an additional comparison.

The best agreement with in-situ measurements of the inner wall temperature were those from viscous flow obtained through the herein proposed simulation. Although the inviscid flow is not representative of the real phenomenon, results showed that it served as a reasonable reference and that the viscosity was not so important in mathematical modeling. This flowing redounded to be more sensible to the initial temperature than to the modification of flow rate. Viscosity confirms itself as a factor of thermal state keeping in a larger inner portion, despite it decreases as temperature increases. A non-insulated region with reduction of thickness might have caused a thermal instability in inviscid flow on the inner wall in a previous region, as can be found in an entrance region, where there isn't a fully developed flowing, or before a curve, according the behavior described by Santana et all (1997).

6. ACKNOWLEDGEMENT

The authors acknowledge "Programa Pesquisa Produtividade" - Universidade Estácio de Sá for funding this research.

7. REFERENCE LIST

Abd-El-Malek M B and Hanna S N, 1997, Sound Attenuation in a Circular Duct of a Viscous Medium in the Absence of Mean Flow. Journal of Nonlinear Mathematical Physics, 4:1-2, 231-240. Doi: 10.2991/jnmp.1997.4.1-2.37;

Akiyama, M and Cheng, K C, 1974, laminar Forced Convection in the Thermal Entrance Region of Curved Pipes with uniform Wall Temperature. The Canadian Journal of Chemical Enngineering, v 52, pp 234-240;

Bejan A , 1993, Heat Transfer. John Wiley & Sons, Inc, New Jersey;

Bogdevičius M, 2003, Nonlinear dynamic analysis of rotating pipe conveying fluid by the finite element method. Transport, 18:5, 224-228. Doi: 10.1080/16483840.2003.10414101

Çengel Y A, Cimbala, J M, 2015, Mecânica dos fluidos: Fundamentos e Aplicações. 3rd ed. AMGH, São Paulo;

Chapman A J, 1984, Fundamentals of Heat Transfer. Macmillan Publishing Company, New York;

Ciambeli J R P and Fonseca Jr R, 2014, Avaliação computacional da presença de gradiente radial de temperatura no duto 12 pol. oc-05-003-ca entre a RLAM e a base de Camaçari (BACAM). Technical Report CT TEE 204/14, CENPES, Rio de Janeiro;

Czubinski F, Neto M M, Barbosa J R, 2013, Caracterização Experimental do Calor Específico e da Condutividade Térmica de amostras de Óleo. Relatório Técnico de Atividades, Departamento de Engenharia Mecânica, Universidade Federal de Santa Catarina;

Dravid, A N, Smith, K A, Merril, E W and Brian, P L T (1971) Effect of Secondary Fluid Motion on Laminar Flow Heat Transfer in Helically Coiled Tubes. AIChE Journal, v 17, N 5, pp 1114-1122;

Lasauskas, E. and Naujokaitis L., 2009, Analysis of three wing sections. Aviation, 13:1, 3-10. Doi: 10.3846/1648-7788.2009.13.3-10;

Holman J F H (1999) Heat Transfer, ed. 8, McGraw-Hill, São Paulo;

Incropera F P, Dewitt D P, Bergman T L, Lavine A S (2014) Fundamentos da Transferência de Calor e Massa, LTC, Rio de Janeiro;

Maciel E S G (2007) Solutions of The Euler and The Navier-Stokes equations Using The Jameson and Mavriplis and The Liou Steffen Unstructured Algorithms in Three-Dimensions. Engineering Applications of Computational Fluid Mechanics,1:4, 238-252. Doi: 10.1080/19942060.2007.11015196;

Madadi A, Kermani M J & Khazaei H (2015) Improvement of a solution of inviscid compressible flows using a mixed wall boundary condition. Engineering Applications of Computational Fluid Mechanics, 9:1, 126-138. Doi: 10.1080/19942060.2015.1004815;

Ozaki N, Harada I, Tokoi H & Yamanouchi A (1978) Flow Profile Measurements of Gas in a Rotating Cylinder. Journal of Nuclear Science and Technology, 15:11, 843-848. Doi 10.1080/18811248.1978.9735599;

Santana, C W S, Torres E G, Lacerda I S (2005) Ajuste de equações para a viscosidade cinemática de produtos de petróleo em função da temperatura. Proceedings of the Third CBP&DPG, Salvador

Santana, L F M (1997) O problema de Graetz em tubos curvos com raio de curvatura irrestrito. Dissertation, Universidade Federal do Rio de Janeiro

Williams J J R (2007) Free-surface Simulations Using An Interface-tracking Finite-volume Method With 3D Mesh Movement. Engineering Applications of Computational Fluid Mechanics, 1:1, 49-56. Doi: 10.1080/19942060.2007.11015181;

8. RESPONSIBILITY NOTICE

The authors are the only responsible for the printed material included in this paper.